Journal of Chemistry and Technologies, 2026, *34*(2), 590-599

Journal of Chemistry and Technologies

pISSN 2663-2934 (Print), ISSN 2663-2942 (Online).

journal homepage: http://chemistry.dnu.dp.ua
editorial e-mail: chem.dnu@gmail.com

UDC 542.9 + 538.221

STRUCTURAL, MAGNETIC, THERMAL AND ABSORPTION CHARACTERISTICS OF Co–Fe ALLOY/COBALT FERRITE COMPOSITES

Liliya A. Frolova[1*], Volodymyr O. Kotsiubynskyi[2], Oleksandr I. Kushnerov[3], Yurii S. Hordieiev[1]

[1]*Ukrainian State University of Science and Technologies, 8 Nauky Ave., Dnipro, 49005, Ukraine*
[2]*Vasyl Stefanyk Carpathian National University, Ivano-Frankivsk, 57 Shevchenko Str., Ivano-Frankivsk, Ukraine*
[3]*Oles Honchar Dnipro National University, 72 Nauky Ave., Dnipro, 49010, Ukraine*

Received 15 March 2026; accepted 27 April 2026; available online 20 June 2026

Abstract

Co-Fe/cobalt ferrite composite nanoparticles were synthesized by hydrothermal method in a high-temperature reactor. X-ray diffractometry (XRD), Fourier transform infrared spectroscopy (FTIR), scanning electron microscopy (SEM), vibrational magnetometry (VSM), differential thermal analysis and thermogravimetry (DTA/TG), respectively, were used to characterize the crystal structure, functional groups, particle size, morphology, and magnetic and thermal properties of the obtained samples. Analysis of X-ray phase analysis data showed that the particles have a two-phase structure consisting of spinel and alloy. Structural and magnetic studies confirmed the formation of Co-Fe/cobalt ferrite composite nanoparticles with a crystallite size of approximately 80–100 nm and shape anisotropy. The saturation magnetization was 190 Emu/g. According to the data of differential thermal analysis and thermogravimetry, the composite is oxidized in an argon atmosphere due to the presence of bound water and hydroxyl groups. A pronounced exothermic effect is observed. The microwave absorption properties of the composite were investigated in the X-band (8–12 GHz). The high absorption value indicates that these composites can be used as promising radio-absorbing materials.

Keywords: magnetic nanoparticles; cobalt ferrite; X-ray diffraction analysis; spinel.

СТРУКТУРНІ, МАГНІТНІ, ТЕРМІЧНІ ТА АБСОРБЦІЙНІ ХАРАКТЕРИСТИКИ КОМПОЗИТУ Co–Fe / ФЕРИТ КОБАЛЬТУ

Лілія А. Фролова[1], Володимир О. Коцюбинський[2], Олександр І. Кушнеров[3], Юрій С. Гордєєв[1]

[1] *Український державний університет науки і технологій, просп. Науки, 8, Дніпро, 49005, Україна*
[2] *Карпатський національний університет імені Василя Стефаника, вул. Шевченка, 57, Івано-Франківськ, 76018, Україна*
[3]*Дніпровський національний університет імені Олеся Гончара, просп. Науки, 72, Дніпро, 49010, Україна*

Анотація

Композитні наночастинки на основі Co-Fe / ферит кобальту були синтезовані гідротермальним методом у високотемпературному реакторі. Для характеристики кристалічної структури, функціональних груп, розміру частинок, морфології, а також магнітних і термічних властивостей отриманих зразків були використані рентгенівська дифрактометрія (XRD), інфрачервона спектроскопія з Фур'є перетворенням (FTIR) та скануюча електронна мікроскопія (SEM), вібраційна магнітометрія (VSM), диференціальний термічний аналіз і термогравіметрія (DTA/TG) відповідно. Аналіз даних рентгенофазового аналізу показав, що частинки мають двофазну структуру, що складається зі шпінелі та сплаву. Структурні та магнітні дослідження підтвердили утворення наночастинок композиту Co-Fe / ферит кобальту з розміром кристалітів приблизно 80–100 нм та анізотопією форми. Намагніченість насичення складала 190 А·м^2/кг. Згідно з даними диференціального термічного аналізу та термогравіметрії, композит окислюється в атмосфері аргону через наявність зв'язаної води та гідроксильних груп. Спостерігається виражений екзотермічний ефект. Мікрохвильові поглинальні властивості композиту були досліджені в X-діапазоні (8–12 ГГц). Високе значення поглинання свідчить про те, що ці композити можуть бути використані як перспективні радіопоглинальні матеріали.

Ключові слова: магнітні наночастинки; кобальтовий ферит; рентгеноструктурний аналіз; шпінель.

**Corresponding author: e-mail: 19kozak83@gmail.com*

doi: 10.15421/jchemtech.v34i2.354370

Journal of Chemistry and Technologies, 2026, *34*(2), 590-599

Introduction

Metal-containing composites based on transition metal ferrites have been the subject of numerous studies in recent years due to their unique properties, distinct from those of either metal or ferrite. They exhibit remarkable magnetic properties, diverse chemical properties, good stability, and excellent catalytic performance, making them useful for a growing number of applications in energy, photoelectrochemical cells, photocatalytic CO_2 reduction, batteries, supercapacitors, and fuel cells [1]. Active ultrafine crystalline metal powders are also used as chemisorbents, to intensify powder metallurgy processes, as raw materials in ceramic production, and to create new polycrystalline and structural materials based on iron and its alloys. Most solid-phase methods do not provide sufficient control over particle growth to obtain microparticles of precisely defined composition and uniform size. The use of liquid-phase reactions allows for the regulation of particle morphology [2; 3]. Various synthesis methods have been developed to date, including reduction with hydrazine, borohydride, high-energy milling in ball mills, reduction of metal oxides with carbon monoxide or hydrogen, carbon, or reactive sputtering [4–6].

For example, it was found that hydrogen reduction of nickel-zinc ferrite resulted in the deposition of nickel-rich metal particles, predominantly at grain boundaries. Moreover, mechanical hardness varied significantly across the reaction surface, indicating that both magnetic and mechanical properties depend on the formation of a ferrite/metal nanocomposite. The precipitation of the metallic phase led to an increase in saturation magnetization, but also reduced permeability and increased losses in the magnetic core [7].

Ferrite-based composite nanotubes were also successfully produced by thermal reduction of α-FeOOH nanowires with hydrogen. The nanotubes have a diameter of approximately 100 nm and a length of tens of micrometers. The formation mechanism of Fe-ferrite composite nanotubes is discussed, and it is established that nonequilibrium diffusion between hydrogen and oxygen is responsible for the formation of the hollow internal structure. Due to the high anisotropy of the one-dimensional structure, the coercivity of the composite nanotubes is higher than that of the previously described granular Fe-ferrite composite nanoparticles. Due to improved impedance matching and higher scattering efficiency, excellent microwave absorption properties were achieved in iron-ferrite composite nanotubes, with a maximum reflection loss of −18 dB and an effective absorption bandwidth (< −10 dB) spanning the entire frequency range of 12.5–17.5 GHz. [8]

Cobalt ferrite nanoparticles of varying stoichiometry, synthesized via sol-gel autocatalytic combustion, were used as the starting material for the production of highly magnetic $Fe_{50}Co_{50}$ and $Fe_{66}Co_{34}$ metallic nanoparticles via topochemical reduction with hydrogen. Structural and magnetic studies confirmed the formation of FeCo nanoparticles with a crystallite size of approximately 30 nm and a magnetization of ~265 A m^2/kg [9].

FeCo–ZnO@C/MWCNT composites were obtained via coordination self-assembly at room temperature followed by controlled carbonization. By precisely controlling the metal molar ratios and carbonization temperatures, the composite achieves a broad effective absorption band (EAB) of 6.8 GHz (11.2–18.0 GHz, matched thickness 1.89 mm) at a low filler concentration of 20 wt.%, as well as a high minimum reflection loss (RL_{min}) of −49.27 dB at 30 wt.%. [10]

The FeSiAl/ferrite flake composite was prepared by a ball mill coprecipitation method. Electromagnetic property measurements showed that the permittivity and magnetic permeability of the FeSiAl flake composites can be tuned by varying the amount of Ni-Zn ferrite. Controllable dielectric losses were observed, which enhance microwave absorption due to the interface between the FeSiAl and ferrites. This enhanced microwave absorption by FeSiAl flake composites is due to the synergy of the metal-ferrite interface and dielectric matching. At a ferrite content of 8 wt.%, enhanced microwave absorption is achieved with a reflection loss of -29.2 dB and a bandwidth of 4 GHz at a matching thickness of 2.5 mm [11].

A wide variety of plasma-chemical processes are used to produce dispersed powders. These include processes based on the reaction of highly volatile metal chlorides with a particular gas; processes in which the working substance is incorporated into electrodes that undergo intense erosion during the plasma process; processes in which plasma jets serve solely as a heat source; and processes involving the introduction of condensed substances into the plasma jet [12].

Highly dispersed iron and oxide particles measuring 10–100 nm can also be produced by sublimation followed by condensation [13].

FeCo@CM composites were efficiently fabricated using advanced microwave plasma-assisted chemical vapor deposition (MPARCVD) technology, providing high efficiency, low cost, and energy savings. The layered FeCo structure exhibits superior properties compared to its spherical counterpart, providing a higher number of open edges and enhanced catalytic activity, which facilitated the deposition of uniform and low-defect graphitized carbon microspheres. As a result, the dielectric loss of the FeCo@CM composites was significantly improved due to increased electrical conductivity and the formation of a large number of heterogeneous interfaces. At a filler content of 40 wt% and a frequency of 7.84 GHz, the FeCo@CM composites achieved a minimum reflection loss of −58.2 dB with an effective absorption bandwidth (f_E) of 5.13 GHz [14].

The carbon-containing material was obtained by electrical explosion of a wire in a polyethylene cavity, and the FeCo/graphene composite was synthesized in a single step. The influence of explosion parameters on the composition, structure, electromagnetic parameters, and impedance matching ability of FeCo/graphene was studied by varying the mass fraction of the feedstock and the input energy in the experimental parameters. At a 20% fill volume and a thickness of 1.5 mm, the maximum reflection loss is −59.05 dB. At a thickness of 1.4 mm, the effective absorption band reaches 4.52 GHz, concentrated in the Ku-band. The results show that anchoring FeCo nanoparticles on the surface of graphene nanosheets enables control of the permittivity over a wide range at low fill levels, which can enhance conductivity loss, interface polarization, and magnetic energy storage capabilities, thereby optimizing impedance matching and loss mitigation [15].

Methods for producing particles from solution are also of interest. A new type of magnetic material, MFe_2O_4/Fe (M = Zn, Mg), with controlled grain sizes and shapes was fabricated on an iron substrate using mild solution processing at temperatures below 200 °C. The cooperative magnetic properties of ferritic-Fe composite thin films were found to be significantly improved compared to single-phase ferrite products, and ferritic-Fe thin films exhibited superparamagnetism [16].

Also, composites consisting of iron- and chromium-doped magnetite were prepared by precipitating metal chloride salts in a KOH solution in a highly alkaline solution. The higher the chromium content, the smaller the lattice parameter and the lower the metal fraction. At Cr/Fe ≤ 0.1, the chemical formula of the composites can be written as $Fe_A/(Fe^{v+}{}_xCr^{3+}{}_{y\_\ 3-(x+y)}O_4)_{1-A}$ $0 \le y \le 0.23$. The two phases, metal and spinel, were found to be intimately mixed within the nanometer-sized particles. At Cr/Fe ratios above 0.1, a hydroxide phase was also present [17]. An isomorphic α-Mn iron-cobalt alloy containing 28 at.% Fe was observed in a metal oxide composite synthesized in an aqueous medium at temperatures below 130 °C. The oxide was a cobalt-containing magnetite. The metal had two structures: an α-Mn structure and a bcc (α-Fe) structure. Refinement of the powder diffraction pattern using the Rietveld method showed that the α-Mn structure transitioned to a bcc structure above 170 °C [18].

The hydrothermal method was used to obtain FeCo alloys under different reaction times. With the change of reaction time (8 h, 10 h, and 12 h), the alloy phase becomes increasingly pure, the particle size and saturation magnetization (MS) of the alloys increase, but the coercivity (Hc) decreases. At the same time, the morphology of the FeCo alloys gradually changes from irregular small particles to hexagonal star-shaped large particles. At a reaction time of 10 h, FeCo alloys exhibit the highest attenuation coefficient (α), excellent impedance matching and microwave absorption characteristics. With a matching layer thickness of 1.95 mm, the minimum return loss (RLmin) at a frequency of 11.12 GHz is −49.88 dB. With a matching layer thickness of 1.56 mm, the maximum effective absorption bandwidth (EAB_{max}) is 6.8 GHz (11.2–18 GHz) [19]. Six bimetallic FeCo particles were also synthesized using hydrothermal synthesis with hydrazine hydrate as a reducing agent at specific Fe:Co ratios. Particles synthesized at a 1 : 1 Fe : Co ratio had a pyramidal shape with small spinel structures. In contrast, particles synthesized at 3 : 1 and 9 : 1 Fe:Co ratios had a flower-like morphology with dimensions of approximately 10 μm, while particles synthesized using pure cobalt salts acquired a palm-branch appearance. Furthermore, thermal stability studies revealed that FeCo alloy particles exhibit greater resistance to oxidation in air compared to pure cobalt particles. Magnetic studies revealed that all particles are paramagnetic materials, with their magnetic properties depending on their composition. Notably, particles synthesized using synthetic mixtures in 1 : 1 and 3 : 1 ratios exhibited the highest saturation magnetization of

Journal of Chemistry and Technologies, 2026, *34*(2), 590-599

151.80 emu g^{-1} and the lowest saturation magnetization of 62.79 emu g^{-1}, respectively [20].

New advanced, environmentally friendly and cost-effective manufacturing technologies are also emerging. Using a dry particle coating method, novel soft magnetic composite materials consisting of iron coated with Ni-Zn/Cu-Zn soft ferrite powder were obtained. The sufficiently high electrical resistivity also ensured relatively low power loss at high frequencies [21].

FeCo-based magnetoelectric composite nanostructures were developed using confinement engineering, achieving a strong absorption capacity of –47.4 dB and a wide bandwidth of 7.10 GHz in a small thickness of 1.9 mm. The exceptional absorption characteristics are due, on the one hand, to the formation of well-dispersed FeCo nanoparticles with a quasi-single-domain size, which leads to enhanced magnetic anisotropy and high-frequency magnetic resonance. On the other hand, the formation of a spatially confined ferrimagnetic phase of $CoFe_2O_4$ reduces magnetic dilution, effectively improving dielectric polarization and impedance matching due to their semiconducting properties [22; 23].

This paper discusses the hydrothermal synthesis of Co–Fe alloy/cobalt ferrite composites and the study of the properties of metal-ferrite composites using microscopy, spectrometry, X-ray diffraction, thermogravimetric analysis, and resonance methods.

Experimental

$FeSO_4 \cdot 7H_2O$, $CoSO_4 \cdot 7H_2O$, and sodium hydroxide were used to prepare the initial solutions. To obtain the composites, 0.5 M $FeSO_4$ and 0.5 M $CoSO_4$ solutions were used. They were mixed in a 2 : 1 iron to cobalt molar ratio. A 1 M NaOH solution was then slowly added to the resulting solution, and the pH of the solution was adjusted to 12.0–12.2. The resulting colloidal solution was placed in a 300 ml Teflon beaker, which was then maintained in a hydrothermal reactor at 250 °C for 4 hours. The precipitate was then washed until a negative sulfate ion reaction was detected and dried at 180 °C.

The morphology of the resulting nanoparticles was studied using a JSM-6390LV scanning electron microscope (SEM) equipped with an X-Max 50 energy-dispersive detector (EDS) (Oxford Instruments Analytical, Oxford, UK).

Also, using the EXPERT 3L X-ray fluorescence analyzer, the mass fractions of elements in composites were determined, with detection limits of 1–10 ppm. A 300×150×240 mm chamber was used, samples weighing 0.01 g. Helium purging was used to increase sensitivity to "light" elements.

The phase composition and structure of ferrite samples were studied using a Shimadzu XRD-7000 X-ray diffractometer with Cu-Kα. radiation.

The study of the thermal properties of samples in an argon atmosphere was carried out using a NetzschJupiter STA-449-F3 thermal analyzer.

The study of the thermal properties of samples in an air atmosphere was carried out on a Derivatograph Q-1500 device (Hungary) of the Paulik-Paulik-Erdei system. The mass of the samples was 0.1 g. The study was carried out in dynamic mode. The heating rate was 10 °C / min. to 1000 °C. Al_2O_3 was used as a reference substance.

The magnetic properties of the samples were studied using a vibrating magnetometer.

Measurements of the absorption coefficient, reflection coefficient for composites were performed using a setup consisting of a G4-83 generator, a S4-11 spectrum analyzer, and a biconical resonator. Measurements were performed at a frequency of 10^8–10^{12} Hz at a temperature of 20 °C.

Results and Discussion

Morphology and structure of composite.

Morphological studies using a scanning electron microscope (SEM) provided a complete picture of the composite surface. The SEM image demonstrating the surface morphology and grain size is shown in Figure 1a. The particles were found to be spherical in shape and 80–100 nm in size. The particles were uniformly distributed and slightly agglomerated due to stronger interactions between the spherical magnetic particles. A characteristic EDX spectrum is shown in Figure 1b. Traces of impurities and other elements were not detected. The samples were also analyzed using an X-ray fluorescence analyzer to determine the Co:Fe ratio (Table 1). Sample K1, synthesized in a hydrothermal reactor, and sample K2, processed at 1000 °C under an argon atmosphere, were analyzed. Figure 1b shows the EDX spectrum of sample K1. The spectrum confirmed the presence of Fe and Co in the sample. The Co/Fe values determined in the ferrite portion of composite K1 are lower than those in the original solution. Since the composites consist of two components—ferrite and metal—this may be due to the uneven distribution of the elements. As can be seen from Table 1, after annealing in an argon

Journal of Chemistry and Technologies, 2026, *34*(2), 590-599

atmosphere at 1000 °C, once the cations are completely incorporated into the crystal lattice, the cation ratio equalizes to stoichiometric.

X-ray diffraction studies of composites K1 and K2 were carried out (Fig. 2).

Table 1

EDXRF analysis of composite nanoparticles K1 and K2

Conditions	Hydrothermal synthesis	Heating 1000 °C in argon
Element	Amount (weight %)	Amount (weight %)
Fe	52.88	47.61
O	24.53	27.28
Co	22.59	25.12
Formula	$CoFe_{2.466}O_4$	$CoFe_{1.999}O_4$

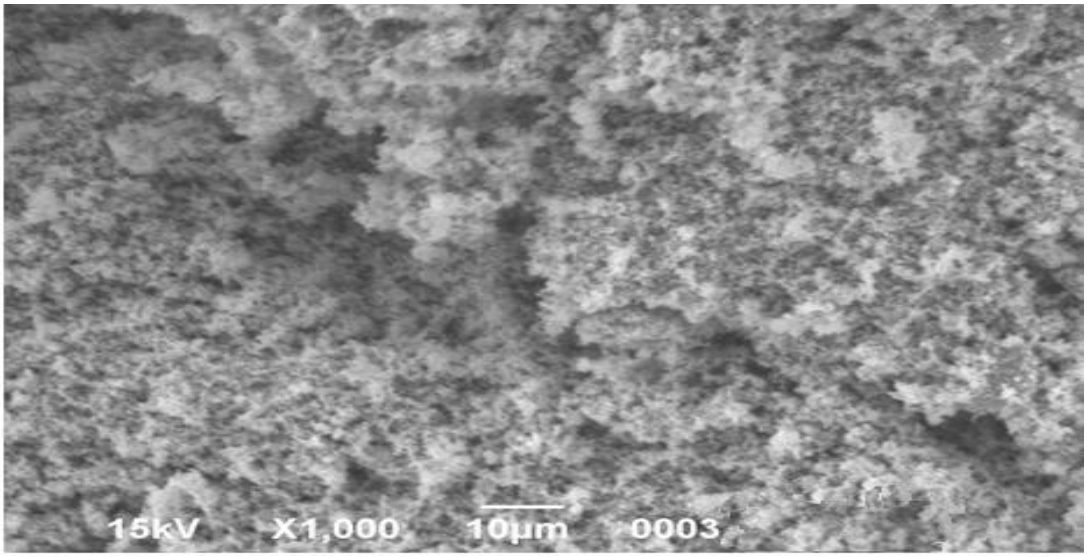

a

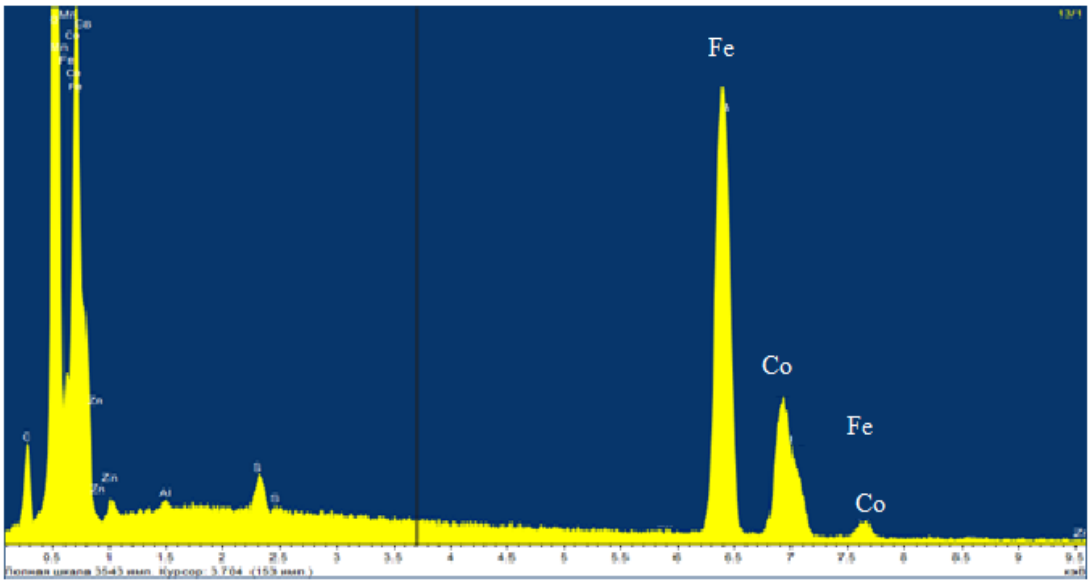

b

Fig. 1. SEM images of the sample K1 (a), EDX spectra of sample K1 (b)

Journal of Chemistry and Technologies, 2026, *34*(2), 590-599

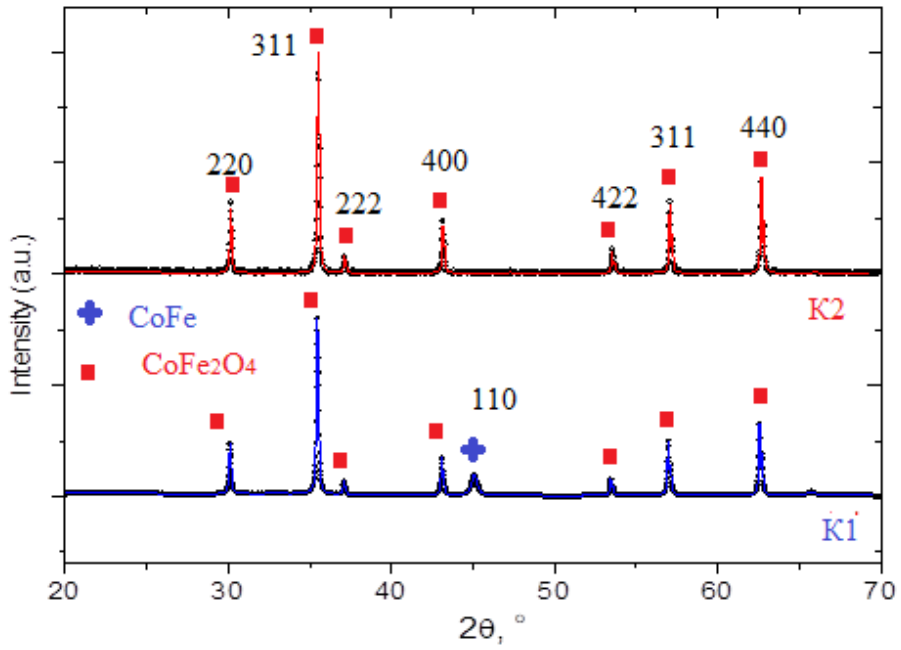

Fig.2. X-ray pattern for samples K1 (hydrothermal synthesis) and K2 (hydrothermal synthesis and annealing at 1000 °C in argon)

The diffraction patterns of samples K1 (hydrothermal synthesis) and K2 (annealing at 1000 °C in argon) indicate that in both cases the cubic spinel phase of cobalt ferrite $CoFe_2O_4$ (space group $Fd\bar{3}m$ describing the face-centered cubic lattice.) dominates, however, heat treatment changes the phase purity, degree of ordering and lattice parameter. For the original sample K1, Rietveld analysis shows the presence of $CoFe_2O_4$ and a crystalline alloy of CoFe (space group $Im\bar{3}m$ describing the body-centered cubic lattice), provided that about 19 % of the material is in a state close to X-ray amorphous, which is consistent with the idea of hydrothermal synthesis, when intermediate phases can be preserved alongside the main one.

The influence of defects and microstresses in the $CoFe_2O_4$ particles is likely. After annealing (sample K2), the phase picture is simplified – 100 % $CoFe_2O_4$ is fixed, the CoFe alloy phase is not isolated, which means its complete inclusion in the spinel structure. For the annealed sample, the disappearance of the CoFe alloy is accompanied by the growth of crystallites and the rearrangement of the defect structure. A change in the unit cell parameter is observed: for K1, a ≈ 8.3942 Å was obtained, while after annealing a ≈ 8.3824 Å.

The decrease in the lattice parameter after high-temperature treatment is explained by the removal of internal stresses, dehydration, and also the redistribution of cations between the tetra- and octa-positions of the spinel (changes in the degree of Co/Fe inversion), which is typical for $CoFe_2O_4$ during heat treatment [24]. After annealing, the total fraction of the "peak" component of the profile increases, and the fraction of the background decreases (38.26 % → 30.80 %), which clearly indicates an increase in crystallinity and a decrease in the content of the nanocrystalline component characteristic of hydrothermally obtained materials. At the same time, the quality of the fit remains comparable: R-Bragg decreases (13.2 → 11.6), and χ^2 changes within acceptable limits (1.9 → 2.4).

A detailed analysis of the peaks corresponding to the CoFe alloy confirms that the lattice parameter is slightly lower than for iron (2.84417 Å compared to 2.8605 Å) and the peaks are shifted along the axis to the region of larger angles. In the Co–Fe alloy system, a decrease in the lattice parameter is observed with increasing Co content, despite comparable atomic radii of the constituent elements. This behavior is explained by electronic and magnetic effects, including enhanced d-band hybridization and stronger interatomic bonds, which lead to lattice compression. As a result, the experimental lattice parameters exhibit a deviation from Vegard's law. Alloys in the ordered state have a slightly larger lattice parameter compared to the disordered state [25].

This corresponds to the formation of a CoFe alloy with a bcc structure. Analysis of the "composition-lattice parameter" diagram [25] also showed that the Co/Fe ratio in the alloy is 7/3.

Journal of Chemistry and Technologies, 2026, *34*(2), 590-599

Table 2

Structural properties of samples K1 та K2

Condition		150 °C	1000 °C argon
Formula sum	$CoFe_2O_4$	Co7Fe3	$CoFe_2O_4$
Entry number	96-153-5821	48-1818	96-153-5821
Total number of peaks	72	12	72
Space group	Fd $\bar{3}$m	Im $\bar{3}$m	Fd $\bar{3}$m
Crystal system	cubic	cubic	cubic
Unit cell	a_t= 8.4000 Å	a_t= 2.8410 Å	a= 8.4000 Å
Unit cell calc.	a_c≈8.3942 Å	a_c≈2.84417 Å	a≈8.3824 Å
I/Ic	5.77	13.12	5.77
Calc. density	5.258 g/cm^3	7.924 g/cm^3	5.258 g/cm^3
Refinement method	Rietveld	Rietveld	Rietveld
R-Bragg, %	13.2	10,1	11.6

Since the composite consists of an alloy and ferrite containing Fe^{2+} cations, oxidation in air is possible upon heating. The results of thermal studies of sample K1 in air are presented in Fig. 3. The DTA curve exhibits two low-temperature effects (90–140 °C), which are accompanied by weight loss. These effects correspond to the release of adsorbed water. As the temperature increases to 400 °C, an exothermic effect associated with the onset of iron oxidation is observed. Weak exothermic effects with maxima at 342, 440, and 575 °C correspond to iron oxidation processes and are smoothed out by the endothermic effects of dehydration and dehydroxolation of ferrite. The surface layer of the composite oxidizes at a temperature of 60–70 °C.

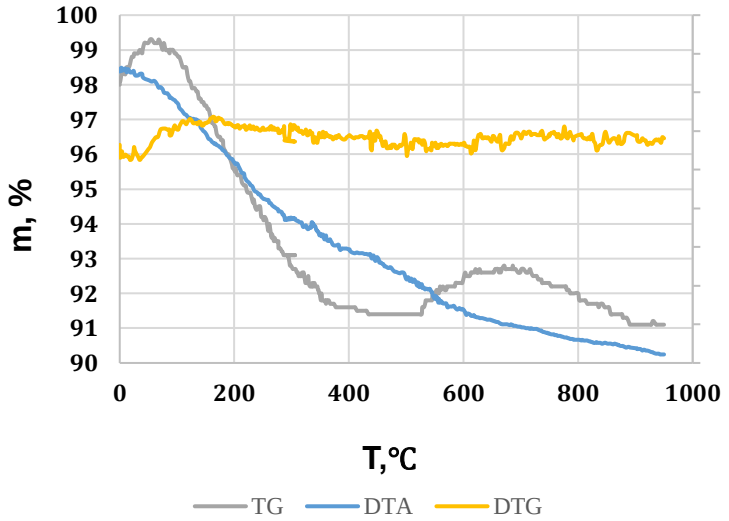

Fig. 3. Results of thermal analysis of sample K1 in air atmosphere

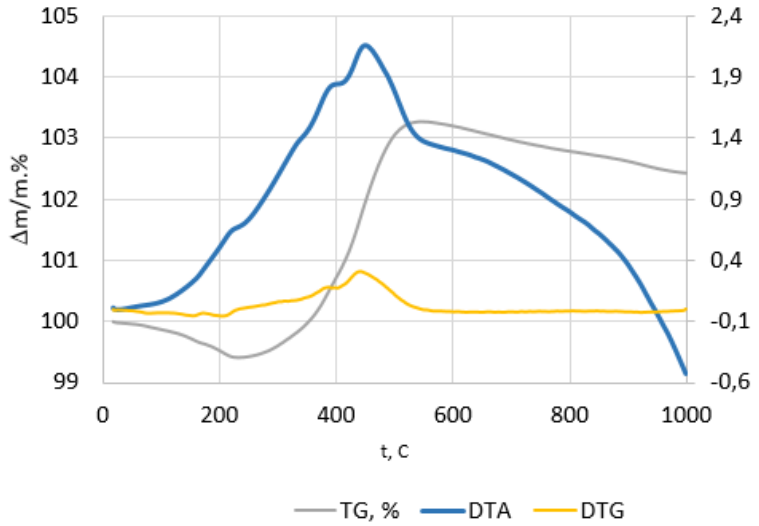

Fig. 4. Results of thermal analysis of sample K1 in argon

Journal of Chemistry and Technologies, 2026, *34*(2), 590-599

Thermal research was also carried out in an argon atmosphere. Figure 4 shows the DTA, DTG, TG curves of the K1 composite. As shown in Fig. 4, several exothermic processes were detected during heating. A broad peak starting at approximately 122 °C is observed. This peak is associated with the removal of internal stresses, since phase transformations were not detected in X-ray diffraction studies. Two exothermic peaks above 380 °C (383, 453 °C) correspond to the processes of crystallization and partial oxidation of the alloy on the surface, which is confirmed by an increase in the weight of the sample, which is confirmed by an increase in the weight of the sample by 3 %. The oxidation process in an inert atmosphere is explained by the hydrothermal synthesis of samples and the presence of adsorbed and crystallization water.

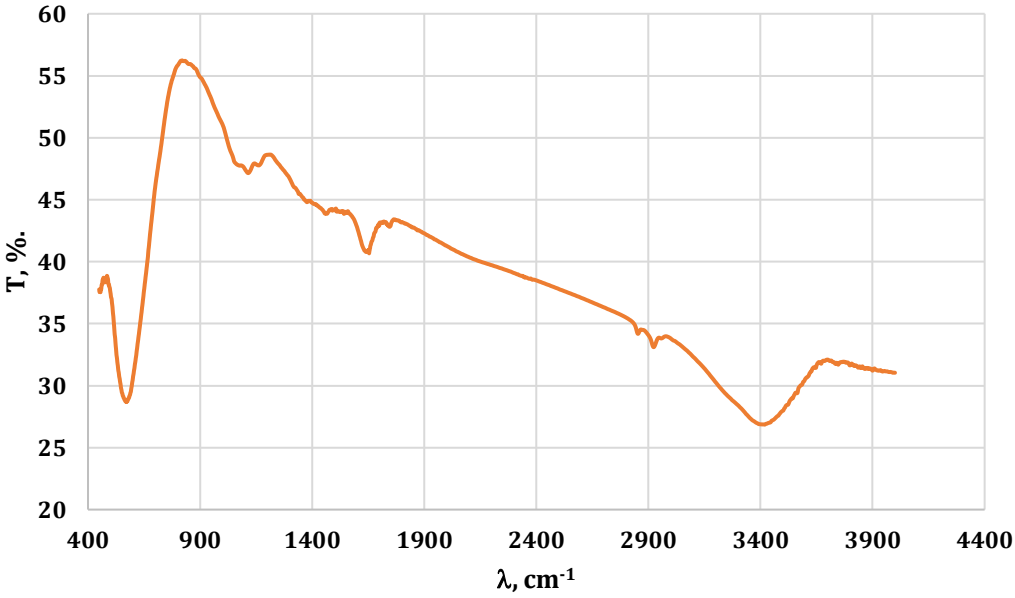

Fig. 5. FTIR spectrum of composite K1

The IR spectra of the synthesized sample in the range of 400–4400 cm^{-1} confirm the results of derivatographic analysis (Fig. 5). Peaks corresponding to both bound and adsorbed water molecules on the surface are present, which is typical for ferrites obtained at low temperatures using hydrophase methods. The peak at 1651–1675 cm^{-1} and a broad band in the range of 3000 and 3500 cm^{-1} are attributed to the stretching and bending vibrations of hydroxyl groups, indicating the presence of water molecules adsorbed on the composite surface. The characteristic peak at 512–595 cm^{-1} corresponds to the natural stretching vibrations of the metal-oxygen bond in the tetrahedral position.

Magnetic Properties.

The hysteresis loop was measured at room temperature (Fig. 6). The presented curve of magnetization (M) versus magnetic field (H) exhibits a slightly narrowed hysteresis loop with two distinct sigmoidal branches and a narrow central part near H = 0. This behavior confirms the presence of two magnetic phases in the composite. It is obvious that cobalt ferrite with high coercivity is responsible for the wider parts of the loop at high fields and the overall hysteresis behavior. The metallic phase dominates the steep central part near H = 0, providing a fast, change in magnetization. This shape of the loop is typical for core-shell nanocomposites, i.e. the $CoFe/CoFe_2O_4$ nanocomposite. At standard temperature, the metallic fraction reacts almost instantaneously and linearly at low fields, providing a steep central slope. The ferromagnetic fraction is magnetized only at higher fields, so broad "shoulders" and a saturation tail are observed.

Absorption Properties of the Composite.

Figure 7 shows the absorption characteristics of the Co–Fe alloy/cobalt ferrite composite in the radar range from 8 GHz to 12 GHz. It is evident that the composition and structure of the composite have a clear impact on its microwave absorption properties. The composite achieves a maximum absorption value of –13.1 dB in the range from 8 GHz to 11 GHz. Significant absorption losses are observed throughout the entire measured range.

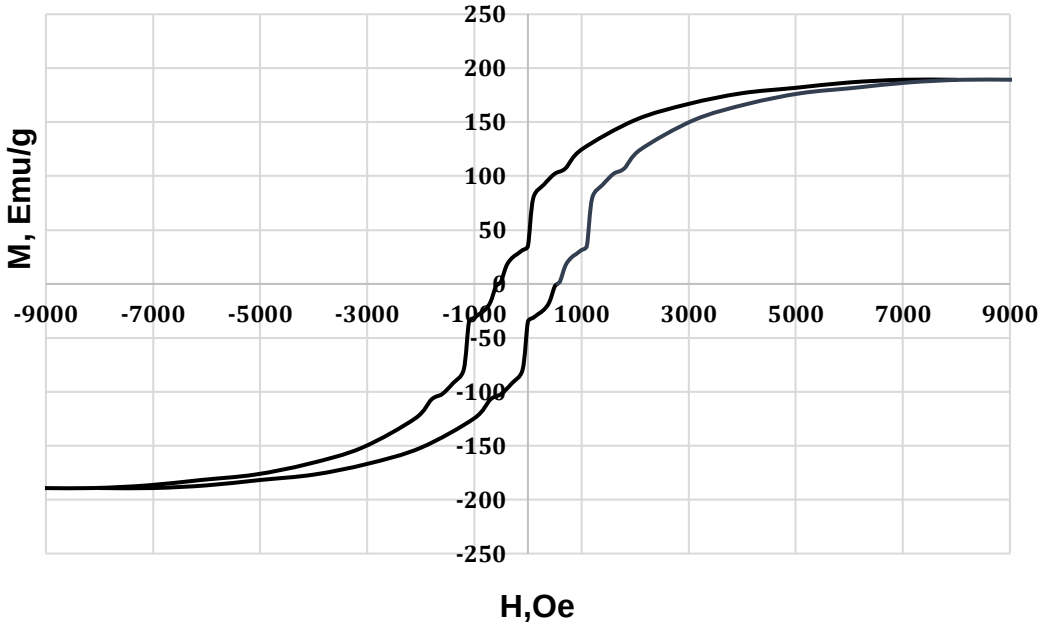

Fig. 6. Field dependence of magnetization of composite K1

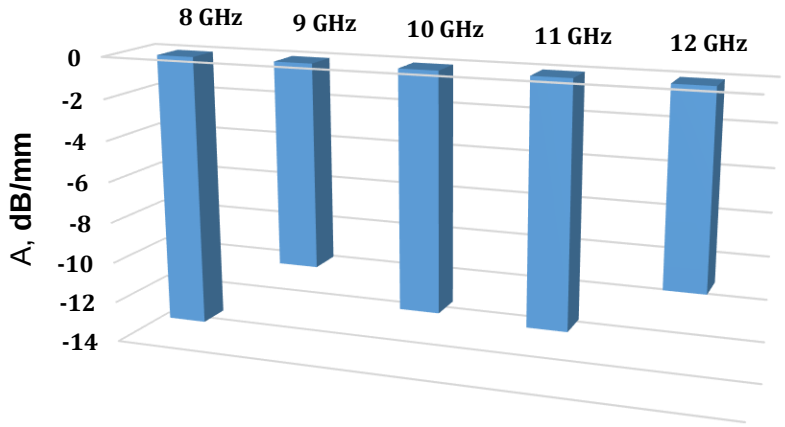

Fig. 7 Absorption characteristics of the K1 composite in the 8–12 GHz range

Conclusions

A Co–Fe alloy/cobalt ferrite nanocomposite was obtained by hydrophase synthesis in a high-temperature reactor. Its magnetic, structural, thermal, optical, and absorption properties were studied using various methods. The phase and elemental composition, purity, stability, and morphology of the composite were also analyzed. The final results showed that the composite particles are spherical. They exhibit higher magnetic properties compared to pure $CoFe_2O_4$ nanoparticles due to the presence of a $Fe_{0.33}Co_{0.67}$ alloy shell.

Furthermore, according to differential thermal analysis and thermogravimetry, the composite oxidizes in an argon atmosphere due to the presence of bound water and hydroxyl groups. A pronounced exothermic effect is observed.

The microwave absorption properties of the composite were studied in the X-band (8-12 GHz). The composite demonstrated a high absorption efficiency of –12…–13 dB. The high absorption value suggests that these composites can be used as promising radar absorbing materials.

References

[1] Abdulwahab, K. O., Khan, M. M., Jennings, J. R. (2024). Ferrites and ferrite-based composites for energy conversion and storage applications. *Critical Reviews in Solid State and Materials Sciences*, *49*(5), 807–855. https://doi.org/10.1080/10408436.2023.2272963

[2] Mamarakhimov, K. M., Sirojev, K. K. (2021). Development of Technologies for Obtaining Metal

Powders (Iron) from Production Waste and Studying Their Properties. *Nanosistemi, Nanomateriali, Nanotehnologii*, *19*(4), 779–798.

[3] Yu, S. H., Yoshimura, M. (2002). Ferrite/metal composites fabricated by soft solution processing. *Advanced Functional Materials*, *12*(1), 9–15. https://doi.org/10.1002/1616-3028(20020101)12:1

[4] Torres, F., Amigó, R., Asenjo, J., Krotenko, E., Tejada, J., Brillas, E. (2000). Electrochemical route for the synthesis of New nanostructured magnetic mixed oxides of Mn, Zn, and Fe from an acidic chloride and nitrate medium. *Chemistry of Materials*, *12*(10), 3060–3067. https://doi.org/10.1021/cm001043h

[5] Lavrenko, V. A. (2002). Preparation and properties of iron powder plated with nickel and cobalt. *Powder Metallurgy and Metal Ceramics*, *41*, 342–346. https://doi.org/10.1023/A:1021104723811

[6] Yang, J. M., Tsuo, W. J., Yen, F. S. (1999). Preparation of ultrafine nickel ferrite powders using mixed Ni and Fe tartrates. *Journal of Solid State Chemistry*, *145*(1), 50–57. https://doi.org/10.1006/jssc.1999.8215

[7] Mullurkara, S., Tan, S., Bracken, C., Wewer, L., Mandal, D., Ohodnicki, P. (2025). Novel soft magnetic metal-ferrite nanostructured ceramic matrix composites (NCMCs) with enhanced saturation magnetization. *Journal of Alloys and Compounds*, *1014*, 182487. https://doi.org/10.1016/j.jallcom.2025.182487

[8] Gong, Y. X., Zhen, L., Jiang, J. T., Xu, C. Y., Wang, W. S., Shao, W. Z. (2011). Synthesis of Fe–ferrite composite nanotubes with excellent microwave absorption performance. *CrystEngComm*, *13*(22), 6839–6844. https://doi.org/10.1039/C1CE05397C

[9] Omelyanchik, A., Varvaro, G., Maltoni, P., Rodionova, V., Murillo, J. P. M., Locardi, F., Peddis, D. (2022). High-moment FeCo magnetic nanoparticles obtained by topochemical H2 reduction of Co-ferrites. *Applied Sciences*, *12*(4), 1899. https://doi.org/10.3390/app12041899

[10] Sun, K., Bao, Z., Tian, J., Yang, P., Wang, Z., Zeng, X., Fan, R. (2025). MOF-derived FeCo-ZnO@C/MWCNT composites featuring multi-level interfaces for broadband microwave absorption. *Carbon*, *234*, 120699. https://doi.org/10.1016/j.carbon.2025.120699

[11] Lei, C., Du, Y. (2020). Tunable dielectric loss to enhance microwave absorption properties of flakey FeSiAl/ferrite composites. *Journal of Alloys and Compounds*, *822*, 153674. https://doi.org/10.1016/j.jallcom.2020.153674

[12] Akhmadullina, N. S., Skvortsova, N. N., Obraztsova, E. A., Stepakhin, V. D., Konchekov, E. M., Letunov, A. A., Shishilov, O. N. (2019). Plasma-chemical processes under high-power gyrotron's discharge in the mixtures of metal and dielectric powders. *Chemical Physics*, *516*, 63–70. https://doi.org/10.1016/j.chemphys.2018.08.023

[13] Shaw, M. G., Humbert, M. S., Brooks, G. A., Rhamdhani, M. A., Duffy, A. R., Pownceby, M. I. (2023). Metal and oxide sublimation from lunar regolith: a kinetics study. *Minerals*, *13*(1), 79. https://doi.org/10.3390/min13010079

[14] Jia, X., Zhang, H., Liu, F., Yi, Q., Li, C., Wang, X., Piao, M. (2024). Exploring the Microstructural Effect of FeCo Alloy on Carbon Microsphere Deposition and Enhanced Electromagnetic Wave Absorption. *Nanomaterials*, *14*(14), 1194. https://doi.org/10.3390/nano14141194

[15] Liang, L., Wu, J., Wang, B., Kong, C., Pervikov, A., Shi, H., Li, X. (2025). Microstructure and electromagnetic wave absorption properties of FeCo/graphene composites prepared by electrical wire explosion method. *Applied Surface Science*, *681factory*, 61577. https://doi.org/10.1016/j.apsusc.2024.161577

[16] Yu, S. H., Yoshimura, M. (2002). Ferrite/metal composites fabricated by soft solution processing. *Advanced Functional Materials*, *12*(1), 9–15. https://doi.org/10.1002/1616-3028(20020101)12:1

[17] Viart, N., Pourroy, G., Grenèche, J. M., Niznansky, D., Hommet, J. (2000). Microstructural and magnetic properties of Fe/Cr-substituted ferrite composites. *The European Physical Journal Applied Physics*, *12*(1), 37–46. https://doi.org/10.1051/epjap:2000169

[18] Pourroy, G., Läkamp, S., Vilminot, S. (1996). Stabilization of iron-cobalt alloy isomorphous of α-Mn in a metal ferrite composite. *Journal of Alloys and Compounds*, *244*(1-2), 90–93. https://doi.org/10.1016/S0925-8388(96)02428-0

[19] Liu, Z., Wang, B., Wei, S., Huang, W., Wang, Y., Liang, Y. (2023). Hydrothermal synthesis of FeCo alloys with excellent microwave Absorption: Effect of reaction time. *Journal of Magnetism and Magnetic Materials, 568,* 170365. https://doi.org/10.1016/j.jmmm.2023.170365

[20] Zhang, C., Liu, Y., Wang, Z., Yang, H. (2024). Characterization of magnetic FeCo particles with controlled bimetallic composition. *Journal of Alloys and Compounds*, *972*, 172744. https://doi.org/10.1016/j.jallcom.2023.172744

[21] Birčáková, Z., Onderko, F., Dobák, S., Kollar, P., Füzer, J., Bureš, R., Dilyova, M. (2022). Eco-friendly soft magnetic composites of iron coated by sintered ferrite via mechanofusion. *Journal of Magnetism and Magnetic Materials*, *543*, 168627. https://doi.org/10.1016/j.jmmm.2021.168627

[22] Lv, H., Zhu, P., Teng, J., Yan, M., Liu, G., Wu, C. (2026). Confinement engineering of FeCo magnetoelectric composite nanocages for enhanced magnetic loss and wideband electromagnetic wave absorption. *Nano Research*, *19*(2), 1104–1112. https://doi.org/10.26599/NR.2026.94908356

[23] Lin, J., Liu, H., Ding, J., Xu, L., Cheng, Z., Gao, F., Zhou, W. (2025). Integration of high-entropy spinel/FeCo magnetic composites with carbon nanotubes for enhanced microwave absorption properties. *Journal of Materials Science: Materials in Electronics*, *36*(23), 1476. https://doi.org/10.1007/s10854-025-15566-5

[24] Caldeira, L. E., Erhardt, C. S., Mariosi, F. R., Venturini, J., Zampiva, R. Y. S., Montedo, O. R. K., Arcaro, S., Bergmann, C. P., Bragança, S. R. (2022). Correlation of synthesis parameters to the structural and magnetic properties of spinel cobalt ferrites (CoFe2O4)–an experimental and statistical study. *Journal of Magnetism and Magnetic Materials*, *550*, 169128. https://doi.org/10.1016/j.jmmm.2022.169128

[25] Sundar, R. S., Deevi, S. C. (2005). Soft magnetic FeCo alloys: alloy development, processing, and properties. *International Materials Reviews*, *50*(3), 157–192. https://doi.org/10.1179/174328005X14339